Article:

Thomas, J.A. orcid.org/0000-0002-8662-7917 (2013) Tuning electronic interactions in mixed valence ruthenium systems incorporating thiacrown ligands. Coordination Chemistry Reviews, 257 (9-10). pp. 1555-1563. ISSN 0010-8545

https://doi.org/10.1016/j.ccr.2012.08.009

Title: Tuning electronic interactions in mixed valence ruthenium systems incorporating thiacrown ligands

Author: Jim A THOMAS
Department of Chemistry, University of Sheffield, Brook Hill, Sheffield, S3 7HF, UK
Email: james.thomas@sheffield.ac.uk.
Telephone: 44 114 222 9325. FAX: 44 114 222 9346.

Abstract: This review outlines the synthesis and properties of mono and oligonuclear polypyridyl ruthenium complexes incorporating a range of S_3 and S_4 thiacrown ligands, focusing on the mixed valence complexes that have been produced in these studies. This work has revealed that the chemical, electrochemical, and electronic properties of the metal centers are modulated by the nature of the coordinated thiacrown ligand. In particular the back-bonding properties of the ligands mean that they strongly stabilize the ruthenium(II) state and also produce metal centers that are relatively kinetically labile. These distinctive electronic properties have been exploited in the construction of mixed valence systems with unusual electrochemical properties and also facilitated the self-assembly of oligonuclear molecular architectures with multiple accessible oxidation states. Computational studies on the isovalent and mixed valence complexes reflect the experimental data by indicating that ,within a series of S_4 coordinated dinuclear complexes, the properties of the mixed valence state are subtly dependent on the cavity size of the coordinated thiacrown.

1. Introduction

Since the original report on the synthesis and optical properties of the The Creutz-Taube (CT) ion [1] $[(NH_3)_5Ru(\mu\text{-pyz})Ru(NH_3)_5]^{5+}$ (where pyz = pyrazine), a huge number of papers on ruthenium based mixed valence, MV, systems have been published [2]. This work has yielded a variety of molecular devices including molecular wires and switches [3 - 7] and also provided insights into the kinetics and thermodynamics of long-range electron transfer [8, 9]. Although these studies have encompassed a wide range of bridging and ancillary ligands, in the vast majority of cases, coordination to ruthenium centers has exclusively involved nitrogen donor sets such as NH_3 and 2,2'-bipyridine (2,2'-bpy). Given that many biological electron transfer (ET) systems are based on transition metals coordinated to sulfur donor sites, my research group decided to investigate how the incorporation of sulfur donating ligands would modulate the ET properties of MV complexes which were analogous to the conventional N-donor systems. In particular, we focused on using thiacrowns shown in Figure 1, as - apart from allowing us to control the number of S-donors in the ligand set - the size of the macrocycle ring provides a method to "fine tune" the coordination geometry around metal centers [10] when they are linked by pyridyl based bridging ligands. Our first step in such studies was to investigate the chemical and electrochemical properties of the $Ru^{II}(9\text{-}S_3)$ fragment, in order to assess whether this moiety would be as a suitable building block towards the synthesis of mixed valence systems.

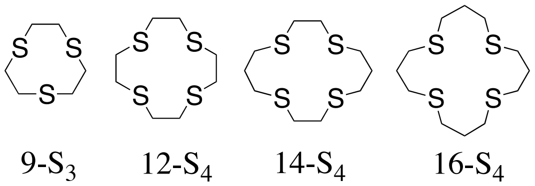

Figure 1 - Thiacrown ligands relevant to this review.

2. Mononuclear complexes with monodentate pyridyl ligands

The complex $[RuCl_2(DMSO)(9\text{-}S_3)]$, **1**, which was first reported by the Sheldrick group [11], seemed to be a suitable starting material for such studies; an investigation into its reaction with a variety of pyridyl-based ligands led to distinctive results – Scheme 1 [12].

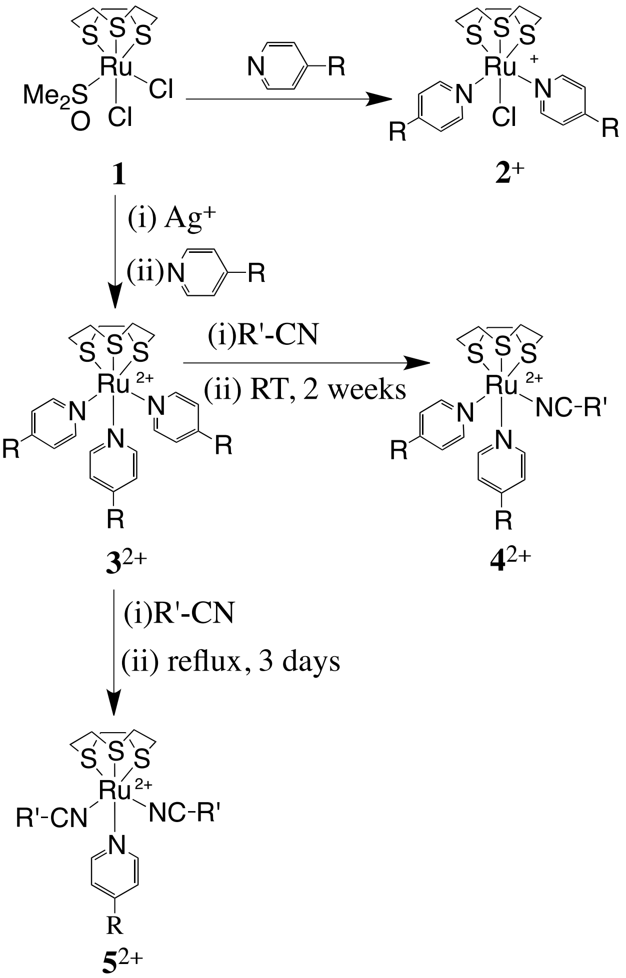

Scheme 1 - Reactions involving monodentate nitrogen donor ligands and the Ru^{II}(9-S$_3$) fragment.

The simple addition of monodentate pyridyl ligands to solutions of **1** led to the isolation of monocationic products such as [RuCl(py)$_2$(9-S$_3$)]$^+$, **2**$^+$ Presumably, the formation of these monocations is due to the restricted ability of thioethers to neutralize positive charges through σ-donation [13,14]. However, pre-treatment of **1** with Ag$^+$ to remove coordinated chloride ligands followed by addition of the relevant pyridyl ligand resulted in the isolation of the dications such as [Ru(py)$_3$(9-S$_3$)]$^{2+}$, **3**$^{2+}$ [12]. It was found that, although the dicationic complexes are stable in poorly coordinating solvents such as nitromethane and dichloromethane, they are unstable towards solvolysis in more coordinating solvents, as illustrated by the fact that over a period of two weeks stirred acetonitrile solutions of $\mathbf{3}^{2+}$ cleanly converted to the dipyridyl complex $[Ru(py)_2(NCMe)(9\text{-}S_3)]^{2+}$, $\mathbf{4}^{2+}$. These substitution reactions precede further under more forcing conditions: for example, after three days refluxing in acetonitrile complex $\mathbf{3}^{2+}$ is cleanly converted into the mono-pyridyl complex $[Ru(py)(NCMe)_2(9\text{-}S_3)]^{2+}$, $\mathbf{5}^{2+}$. Strikingly, related nitrile-based complexes do not display the same reactivity, complexes $[Ru(NCR)_3(9\text{-}S_3)]^{2+}$ (R = Me, Ph) are inert to solvolysis by other coordinating solvents, even over a period of 1 month. Ruthenium(II) complexes incorporating pyridine ligands are often synthesized via nitrile intermediates, but clearly in this case the opposite is true. This unusual reactivity is due to two factors. The crystal structure of $\mathbf{3}^{2+}$ reveals that one face of the complex is steric congested due to interactions between the ortho hydrogens of the coordinated pyridine ligands. It was reasoned that these unfavorable steric interactions are one of the causes of the relative instability of $\mathbf{3}^{2+}$ and explains why the substitution of pyridine ligands stops after the replacement of only two of these ligands. However, the related facially capped complex $[Ru(tpm)(py)_3]^{2+}$ (tpm = tris(1-pyrazole)methane) is stable towards solvolysis [15] and a comparison of its crystal structure with that of $\mathbf{3}^{2+}$ shows that the Ru-py bond lengths in the tpm-based complex are almost 5 pm shorter than those for $\mathbf{3}^{2+}$. These observations indicate that the unusual reactivity of $\mathbf{3}^{2+}$ can also be partially attributed to electronic factors - it is now well established that thiacrown ligands are good π-acceptor ligands with C–S σ* orbitals of appropriate symmetry acting as the acceptors [16]. However, while coordinated monodentate pyridyl ligands are labilized by the $Ru^{II}(9\text{-}S_3)$ moiety, we found that by employing bidentate chelating ligands we could synthesize oligonuclear complexes that displayed much greater kinetic stability, allowing their mixed valence states to be studied.

3. Dinuclear mixed valence $Ru^{II/III}$ systems containing the $9\text{-}S_3$ ligand

To make a detailed comparison between conventional MV systems built up from $[Ru(NH_3)_4]^{2+/3+}$ and $[Ru(2,2'\text{-}bpy)_2]^{2+/3+}$ units, dinuclear complexes bridged by three different bridging ligands were synthesized [17,18]. The bridging ligands 2,3-bis(2-pyridyl)pyrazine (bpp), 2,2'-bipyrimidine (bpym), and (3,6-bis(2-pyridyl)-1,2,4,5-tetrazine (bpta) were selected to vary the intensity of coupling between the metal centers. While the first member of this series is a typical, much employed, bridging ligand in energy and electron transfer systems [19], previous studies have shown that bpym bridged systems often display comparatively weaker electronic and electrochemical coupling [20], whilst studies on bptz-based $Ru^{III/II}$ complexes demonstrated that the low lying LUMO of the central tetrazine bridge can facilitate very intense interactions [21, 22].

The reaction of **1** with the relevant ligands yielded the isovalent dinuclear complexes, $[\{RuCl(9\text{-}S_3)\}_2(bpym)]^{2+}$, $\mathbf{6}^{2+}$, $[\{RuCl(9\text{-}S_3)\}_2(bpp)]^{2+}$, $\mathbf{7}^{2+}$, and $[\{RuCl(9\text{-}S_3)\}_2(bpta)]^{2+}$, $\mathbf{8}^{2+}$ - Figure 2 [17, 18]. The electrochemical interaction between the two ruthenium(II) centers in these complexes was first assessed through cyclic voltammetry.

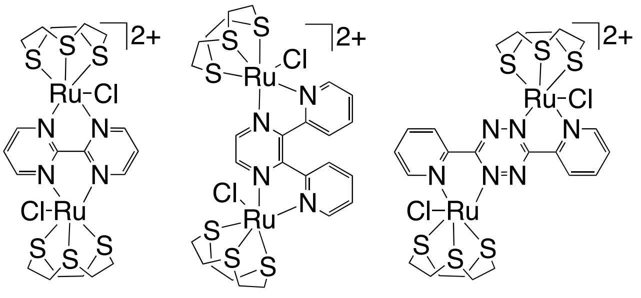

$\mathbf{6}^{2+}$ $\mathbf{7}^{2+}$ $\mathbf{8}^{2+}$

Figure 2 – Structure of complexes $\mathbf{6}^{2+}$, $\mathbf{7}^{2+}$, and $\mathbf{8}^{2+}$.

It was found that although both $\mathbf{7}^{2+}$ and $\mathbf{8}^{2+}$ were oxidised in two clearly defined and reversible one-electron processes, oxidation of $\mathbf{6}^{2+}$ produced two overlapping waves. In all cases, the potentials for the first oxidation of the thiacrown complexes were intermediate to the values for their $Ru^{II}(NH_3)_4$ and $Ru^{II}(2,2'\text{-bpy})_2$ analogues, but closer to the figures obtained for the latter systems. For example, the first oxidation of $\mathbf{8}^{2+}$ was observed at 1.36 V (*vs.* Ag/AgCl), while the potentials of the equivalent couples for the $Ru^{II}(NH_3)_4$ and $Ru^{II}(2,2'\text{-bpy})_2$ complexes were observed at 0.69 V and 1.52 V respectively [21, 22]. These observations indicate that, despite the inclusion of a σ- and π-donor chloride ligand and the lower charge of the $[RuCl(9\text{-}S_3)]^+$ unit, the π-accepting properties of the thiacrown ligand still leads to a great degree of Ru^{II} oxidation state stabilization. A consideration of the difference in the

Ru(1) and Ru(2) oxidation potentials, $\Delta E_{1/2}$, for the complexes revealed a similar trend. The smallest value of $\Delta E_{1/2}$ (120 mV) is observed for the oxidation of **6**$^{2+}$, with the equivalent values for **7**$^{2+}$ and **8**$^{2+}$ being 155 mV and 480 mV respectively. Comproportionation constants, K_c, derived from these data revealed more subtle differences when compared to the N-donor systems.

K_c values for the thiacrown-based complexes are, in all cases, appreciably smaller than those for their $Ru(NH_3)_4$ analogues; this is not unexpected as the inclusion of σ-donor ancillary NH_3 ligands will enhance the metal/bridging-ligand electronic overlap. Somewhat surprisingly, while the large comproportionation constant for **8**$^{2+}$ (1.4×10^8 [17]) is virtually identical to its Ru(2,2'-bpy)$_2$ analogue, K_c values for **6**$^{2+}$ and **7**$^{2+}$ are both lower than their Ru(2,2'-bpy) equivalents [18]. By itself the electrochemical data indicates that interaction between metal centers is weakest in the thiacrown coordinated systems; however, previous studies have shown that electrochemical data do not always give a true indication of actual electronic coupling [23 - 25]. In fact, more definitive information on this issue can be revealed through a consideration of the optical properties of the MV state.

The absorption spectra of **6**$^{3+}$ - **8**$^{3+}$ were probed by spectroelectrochemistry. For all three complexes, generation of the Ru$^{III/II}$ MV state leads to the growth of an near infra-red, intervalence charge transfer (IVCT) band. As might be expected from the electrochemical data, **8**$^{3+}$ displayed a relatively intense IVCT band; and while a broader – but nonetheless well-defined - band was observed for **7**$^{3+}$, for **6**$^{3+}$, a very broad, weak low energy band was only revealed through subtraction of the **6**$^{2+}$ spectrum – Figure 3.

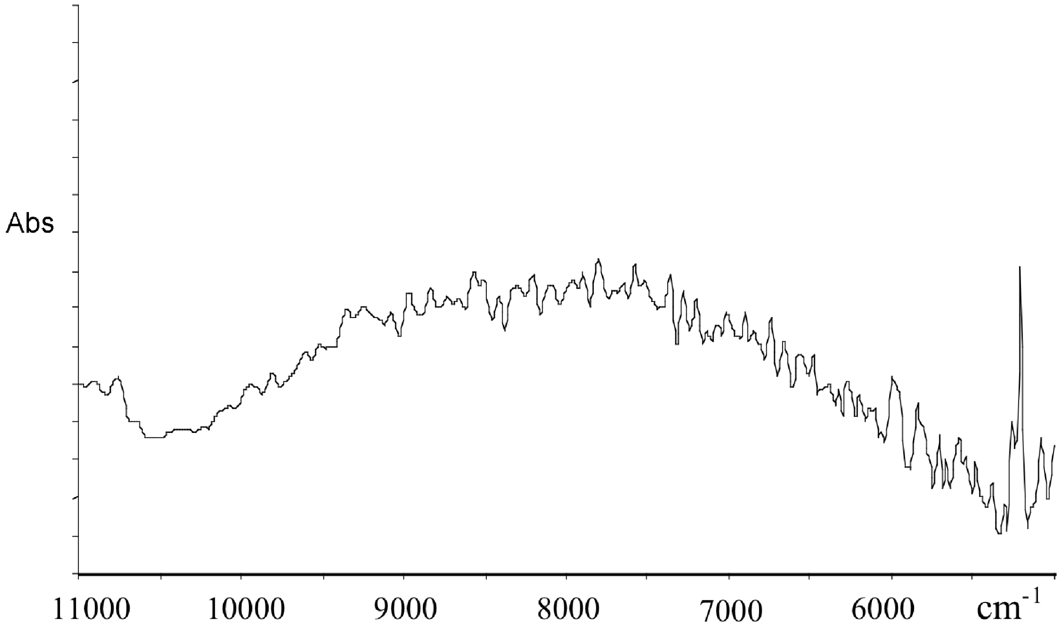

Figure 3 – The [$\mathbf{6}^{3+}$ - $\mathbf{6}^{2+}$] difference spectrum for the NIR region.

These bands were then analyzed through a comparison with the theoretical model for localized, "electron hopping," MV systems developed by Hush [26-28]. It was found that electronic coupling - as estimated by H_{AB} - is considerably larger than indicated by the electrochemical data. Indeed, the analysis revealed that although $\mathbf{6}^{3+}$ is a Robin and Day Class II (valence localized) system [29], $\mathbf{7}^{3+}$ and $\mathbf{8}^{3+}$ are in fact Class III, (valence delocalized) systems, with $\mathbf{8}^{3+}$ displaying coupling comparable to the CT-ion itself [1]. The apparent contradictions between the electrochemical and optical data were resolved through a consideration of the factors that contribute to the free energy of comproportionation ΔG_c:

$$\Delta G_c = \Delta G_r + \Delta G_e + \Delta G_s + \Delta G_i \qquad (1)$$

In this expression ΔG_r is the free energy of resonance, ΔG_e is an electrostatic term that takes into account the mutual repulsion of the two cationic metal centers, ΔG_s is an entropic factor that takes the value (1/2)RT ln 1/4, and ΔG_i is a synergistic effect due to the stabilization of Ru^{II} by Ru^{III} or vice versa [30]. Only ΔG_r is a measure of true electronic coupling. Previous electrochemical studies have demonstrated that ΔG_e is dependent on the charge of the system studied [31]. From these arguments, it would be expected that ΔG_e for $Ru^{III/II}Cl(9\text{-}S_3)$ based complexes will be less than that for more highly charged $Ru^{III/II}(NH_3)_4$ and $Ru^{III/II}(diimine)_2$ systems. It was also suggested that the combination of π-acceptor and π-donor ligands within the RuCl(9-S_3) moiety leads to an enhancement of ΔG_i thus stabilizing both Ru^{II} and Ru^{III} oxidation states and favoring the mixed valence state.

4. Mixed valence $Ru^{II/III}$ metallomacrocycles containing the 9-S_3 ligand

The enhanced kinetic lability of the Ru^{II}(9-S_3) moiety has facilitated the thermodynamic self-assembly of oligonuclear complexes. In such conditions entropic and enthalpic arguments indicate that discrete architectures are favored [32]. In our first report on this approach, we used nitromethane as the non-coordinating solvent and reacted **1** with 4,4'-bpy in an 8:12 stoichiometry. This led to the isolation of an octanuclear cube complex, $\mathbf{9}^{16+}$[33] – Figure 4. Unfortunately, although the Ru^{II} centers display stepwise oxidizations, as for the analogous mononuclear complex $[Ru(4,4'bpy)_3(9\text{-}S_3)]^{2+}$, all these processes were chemically irreversible and thus any MV states could not be investigated. However, related studies on trinuclear metallomacrocycles assembled through a similar approach led to more successful outcomes.

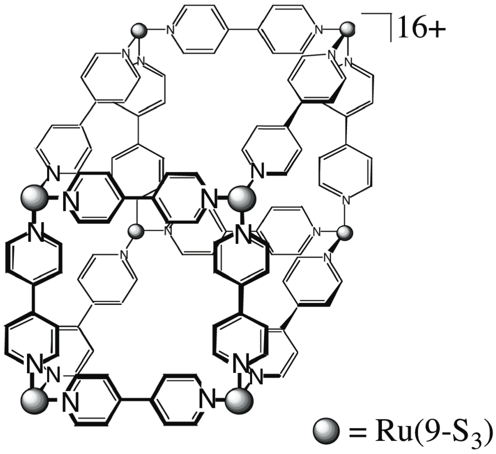

$\mathbf{9}^{16+}$

Figure 4 – Structure of self-assembled cube $\mathbf{9}^{16+}$.

Inspired by the elegant studies of Fish on trinuclear bowls containing cp*Rh^{III} bridged by adenine-based ligands [34], such as $\mathbf{10}^{3+}$, Figure 5, we investigated the reaction of **1** with 9-methyl adenine (9-MA) in a pH7 buffered aqueous solution [35].

Initially we found that the only product of the reaction was in fact the mononuclear complex **11**$^{2+}$, where the exocyclic NH_2 of the coordinated adenine-based ligand has not been deprotonated. It seems that, compared to the cp*Rh^{III} center, the coordinated Ru^{II}(9-S_3) moiety is not a strong enough Lewis acid to cause deprotonation of the amine group. Consequently, the N1 position of 9-MA is an insufficiently good donor to compete for the metal coordination site occupied by DMSO in **11**$^{2+}$ and self-assembly of higher order structures does not occur. Since it is established that coordinated thiacrowns are susceptible to cleavage by nucleophiles [36] the deprotonation by a sterically hindered base was investigated.

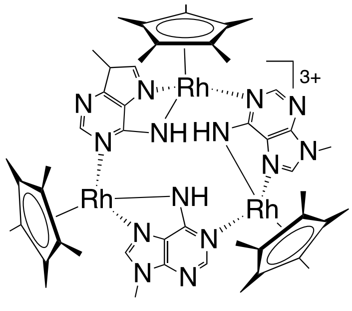

10^{3+}

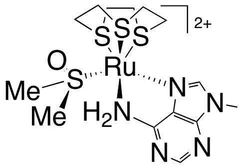

11^{2+}

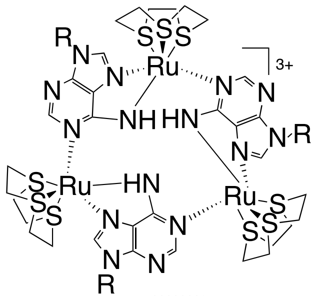

12^{3+}, R = CH_3; **13**$^{3+}$, R =

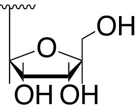

Figure 5 - Structure of metallomacrocycle **10**$^{3+}$, reported by Fish and co-workers, and thiacrown Ru^{II} complexes **11**$^{2+}$, **12**$^{3+}$, and **13**$^{3+}$.

In the presence of pentamethylpiperidine, PMP - a very strong BrØnsted base but a weak nucleophile – the reaction of **1** with 9-MA affords the trinuclear bowl **12**$^{3+}$ as the only product. A consequent study showed that, for suitably hindered adenine bridging ligands, this procedure appears to be general; for example reaction with adenosine yields macrocycle **13**$^{3+}$ [37]. Oxidation of these structures occurs in three reversible processes between 0.8 – 1.4 V. The three couples are most clearly revealed by dI_1/dE *vs*. E deconvolutions of the voltammetry data; this transform produces traces equivalent to a differential pulse polarogram with an additional reverse sweep [38] - Figure 6.

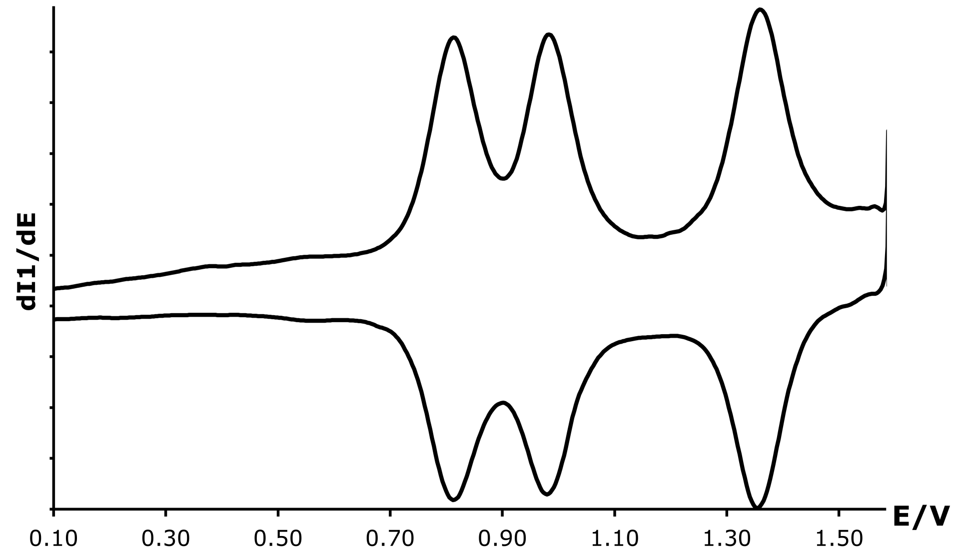

Figure 6 - dI1/dE vs. E deconvolution [38] of the cyclic voltammogram for the oxidation processes of complex **13**$^{3+}$.

A comparison of data for **12**$^{3+}$ and **13**$^{3+}$ revealed that the three oxidation steps occur at almost identical potentials in both complexes. Thus the analysis confirms that the macrocycles have four accessible oxidation states, two of which are formally mixed valence:

$$[Ru^{II}_3]^{3+} \underset{+\,e^-}{\overset{-\,e^-}{\rightleftharpoons}} [Ru^{II}_2Ru^{III}]^{4+} \underset{+\,e^-}{\overset{-\,e^-}{\rightleftharpoons}} [Ru^{II}Ru^{III}_2]^{5+} \underset{+\,e^-}{\overset{-\,e^-}{\rightleftharpoons}} [Ru^{III}_3]^{6+} \tag{2}$$

As shown in Table 1, the comproportionation constant calculated for the [Ru^{II}Ru$_2^{III}$] states are several orders of magnitude larger than that of the [Ru$_2^{II}$Ru^{III}] states, suggesting that the intensity of electronic coupling is different in the two MV states; an inference that was confirmed by absorption spectroscopy studies on the macrocycles.

Table 1 - Comproportionation constants derived from electrochemistry data for the mixed valence states of Ru(9-S_3)-based macrocyclic bowls.

Complex	**$\Delta E_{1/2}$/mV**	**K_c**
12^{4+}	170	760
13^{4+}	165	625
12^{5+}	380	2.75×10^6
13^{5+}	370	1.85×10^6

The spectra of **12**$^{4+}$ and **13**$^{4+}$ are dominated by structured, low energy IVCT bands typically seen in oligonuclear MV systems where a low symmetry coordination geometry, extensive orbital mixing and spin orbit coupling lead to $d\pi^{5/6}$ states being split into Kramer doublets [2]. The relative low intensity and broadness of these bands, as well as a comparison to their theoretical width at half-height, indicated that the [$Ru^{II}_2Ru^{III}$] valence state for both complexes is in an electron hopping state. Contrastingly, electrochemical generation of **12**$^{5+}$ or **13**$^{5+}$ leads to the IVCTs, sharpening, shifting to lower energy, and increasing in intensity. An analysis of these new bands clearly reveals that that the [$Ru^{II}Ru^{III}_2$] state is in fact valence delocalized.

These observations are in contrast with data obtained for conventional trinuclear mixed valence complexes bridged by tritopic ligands complexes [39], where the spacing of electrochemical couples and charge delocalization are approximately constant, as would be expected if there was no variation in the individual metal–metal interactions across the redox series. It was suggested that the anomalous properties of the macrocycles arise from their distinctive molecular architectures. In conventional systems with a central rigid tritopic bridging ligand, redox-induced changes in individual metal-ligand bond lengths and angles are not directly mechanically coupled to the other metal centres within the complex. However, connectivity in the macrocycles is more complex as the metal centers are connected through three peripherally arranged ditopic bridging ligands; hence changes in the bonds and angles at one metal centre may be mechanically coupled to the other two. Therefore structural changes can, in principle, be propagated throughout the macrocycle – Scheme 2, thus affecting orbital mixing within the whole system [37].

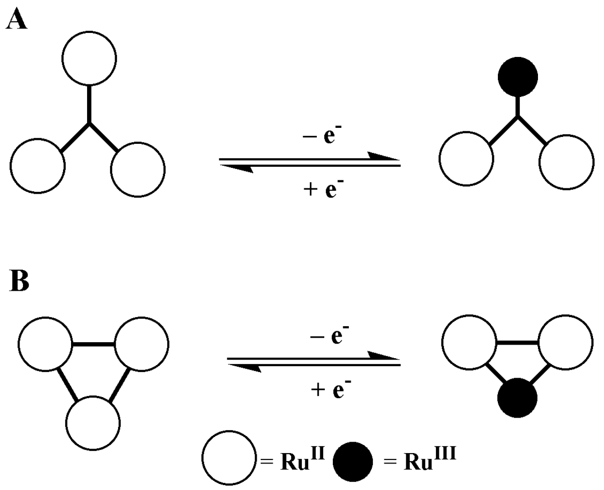

Scheme 2 - Schematic showing effect of oxidising a single metal centre in: (A) a trinuclear complex bridged by a single central ligand. (B) a trinuclear complex where the metal ions are connected by three ditopic ligands. In both cases, it is assumed the final mixed valence state is a Class II system, where bond lengths and angles are *not* averaged

5. Synthesis and NMR fluxionality of mononuclear Ru(n-S$_4$) complexes

To explore the effect of increasing the number of S-donor sites in the ligand set of the ruthenium centers, we set out to synthesize tetrathiacrown-based analogues of **1** as suitable starting materials towards this aim.

The reaction of Ru(DMSO)$_4$Cl$_2$ with n-S$_4$ (where n = 12, 14, and 16) yields monocationic complexes [RuCl(DMSO)(n-S$_4$)]$^+$, which react readily with pyridyl based ligands, but - as with **1 -** the coordinated chloride ligand of these complexes is only substituted after treatment with Ag$^+$ [40, 41]. We initially investigated the properties of simple mononuclear dicationic complexes **14**$^{2+}$, **15**$^{2+}$, and **16**$^{2+}$ containing 2,2'bpy. Crystallographic studies revealed that although complex **14**$^{2+}$ shows considerable distortion away from ideal octahedral coordination geometry [40] due to the small cavity size of 12-S$_4$ complexes **15**$^{2+}$, and **16**$^{2+}$ are much less distorted with **15**$^{2+}$ being the closet to an ideal geometry [41]. This suggested that the orbital overlap between the components of the complexes could be tuned through thiacrown ligand selection.

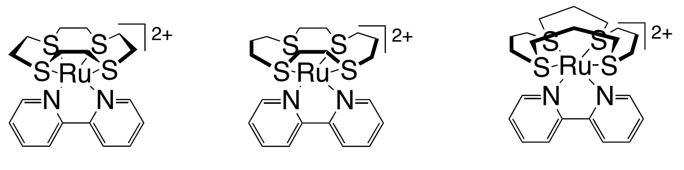

14^{2+} **15^{2+}** **16^{2+}**

Figure 7 – Structures of mononuclear complexes, **14^{2+}**, **15^{2+}** and **16^{2+}**

However, initial NMR studies on the three complexes suggested that they may not be stable in coordinating solvents as they revealed line broadening suggestive of chemical exchange involving cleavage of the Ru—N bonds with 2,2'bpy [40]. Consequent studies on **15^{2+}** showed that at temperatures below -43 °C the broadened signals split to give two sets of signals indicating the presence of two isomers in a ratio of 1.00:0.16. Further detailed COSY and EXSY experiments revealed that the observed exchange broadening is, in fact, due to coordinated sulfur lone pair inversion - that is interconversion between three possible invertomers – Figure 8 [41].

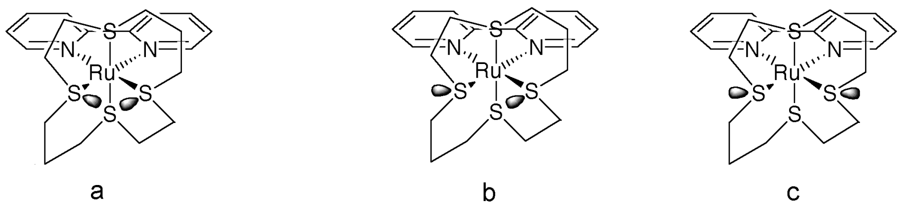

a b c

Figure 8 – The three possible isomers that can arise from the orientation of macrocyclic sulfur lone pair in **15^{2+}**.

Furthermore, a comparison of the data for three complexes indicated that whilst the ***c***-conformer is the most stable invertomer for **14^{2+}**, for complexes **15^{2+}** and **16^{2+}** the ***b***-conformer is preferred. DFT calculations provided a rationalization for these observations as they indicated that the relative stability of the three isomeric forms are related to the number and strength of unfavorable intramolecular contacts within the coordinated macrocycle and between the macrocycle and coordinated 2,2'bpy. Having established the stability of this class of complex, we went on to investigate systems involving ditopic bridging ligands containing both bidentate and monodentate coordination sites.

6. Dinuclear Ru(n-S_4)-based complexes using bridging ligands with bidentate coordination sites.

When dinuclear ruthenium(II) analogues were synthesized it was found that their electrochemical and electronic properties *were* dependent on the nature of the coordinated thiacrown. While the $\Delta E_{1/2}$ (120 – 140 mV) and hence K_c values for the three complexes were similar - suggesting that the MV states are Class II - ligand effects *were* revealed in a closer study of the first oxidizations of $\mathbf{17}^{4+}$ - $\mathbf{19}^{4+}$ [42] – Figure 9. A comparison of this first couple revealed that the most anodic is observed for $\mathbf{17}^{4+}$ while the most easily oxidised complex is $\mathbf{19}^{4+}$, with the oxidation for $\mathbf{17}^{4+}$ being intermediate between these values; these data agree with the optical properties of the complexes.

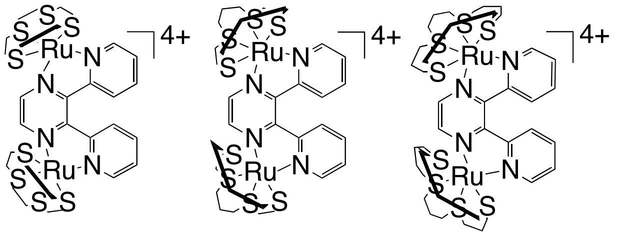

$\mathbf{17}^{4+}$ $\mathbf{18}^{4+}$ $\mathbf{19}^{4+}$

Figure 9 – Structures of dinuclear complexes, $\mathbf{17}^{4+}$, $\mathbf{18}^{4+}$ and $\mathbf{19}^{4+}$

Complexes $\mathbf{17}^{4+}$ - $\mathbf{19}^{4+}$ all display Ru^{II}→bridging ligand-based metal-to-ligand charge-transfer, MLCT, bands. Since each of these complexes has the same bridging ligand (and thus a similar LUMO) any difference in the energy of their MLCT bands can be attributed to perturbation of their metal-based HOMO. Thus, as indicated by the electrochemical data, $\mathbf{19}^{4+}$ has the lowest energy MLCT of three complexes, whilst $\mathbf{18}^{4+}$ has the highest energy MLCT. To investigate such effects in more detail complexes $\mathbf{20}^{4+}$ and $\mathbf{21}^{4+}$ were synthesized [43] so that direct comparisons with $\mathbf{8}^{2+}$ could be made.

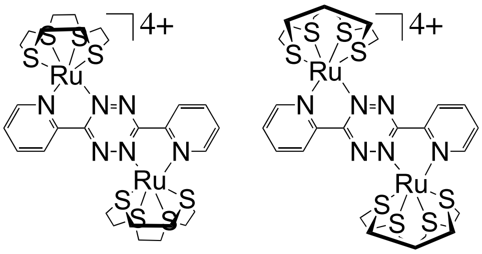

20^{4+} **21^{4+}**

Figure 10 – Structures of dinuclear complexes, **20^{4+}** and **21^{4+}**

Crystal structures of **20^{4+}** and **21^{4+}** showed that – at least in the solid state – both complexes take up conformation ***b***, which is the lowest energy conformation for coordinated 14-S_4 in mononuclear complex **15^{2+}** and only slightly higher in energy than conformation ***c*** for the coordinated 12-S_4 in **14^{2+}**. The most obvious differences between **8^{2+}** and its S_4 analogues were in their electrochemical properties. Although **8^{2+}** clearly displays two Ru^{II}-based oxidations and a low-lying reduction of the tetrazine ring of bpta which - as is typically observed for dinuclear Ru^{II} complexes - is at very low cathodic voltages (-0.049 V vs. Ag/AgCl), for both **20^{4+}** and **21^{4+}** a comparable bpta/bpta$^{\bullet-}$ reduction is not observed. What is more, while the first of the two observed anodic couples is at an unusually low potential of 0.25 – 0.45 V, the second is just at the edge of the MeCN redox window at 1.8 – 1.9 V.

Given the π-acceptor properties of the thiacrown ligand it seemed unlikely that this first oxidation is due to a Ru^{II}-based process, especially as this would also imply that $\Delta E_{1/2}(1,2)$ for **20^{4+}** and **21^{4+}**, would take an unprecedentedly large value of over 1.5 V. Therefore, it was concluded that the first oxidation in the n-S4 systems is actually due to the bpta/bpta$^{\bullet-}$ based couple, shifted by > 0.5 V compared to previously reported Ru^{II}-based systems, and that the second observed anodic process is actually the first metal ion oxidation. These data implies that, in the conditions employed in the CV experiments and at 0 V *vs*. Ag/AgCl, the metal complexes are actually in the **20^{3+}** and **21^{3+}** state and contain a reduced radical anion bridging ligand; they also indicate that the second $Ru^{III/II}$ couple occurs at a potential beyond the MeCN redox window.

When solutions of either **20^{4+}** or **21^{4+}** are placed in anaerobic conditions at 0 V *vs*. Ag/AgCl distinctive changes in their absorption spectra are observed, most notably intense bands at 600 - 800 nm assigned to Ru → bpta ^{3}MLCT transitions almost completely collapse – Figure 11. On application of a potential above the first anodic couple for the complexes, processes that exactly mirror image the initial changes occur, with the original low energy bands growing back in. These observations offer further proof that under an inert atmosphere and at 0 V *vs*. Ag/AgCl, the complexes contain two Ru^{II} centers, bridged by the radical anion, $bpta^{\bullet -}$.

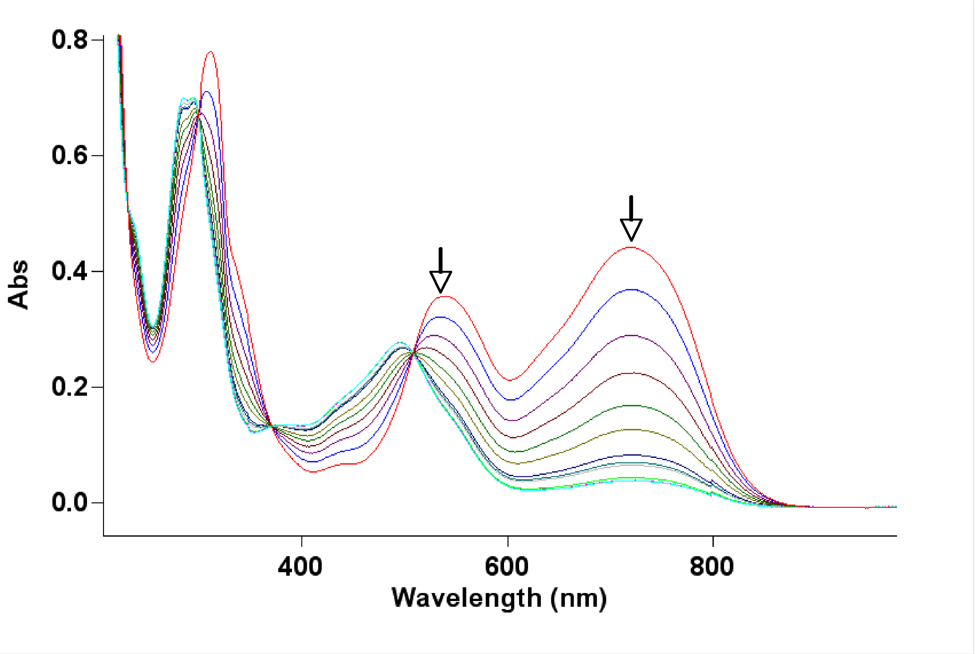

Figure 11 - Absorption changes observed when $\mathbf{21}^{4+}$ is placed in an inert atmosphere at +0.00 V *vs*. Ag/AgCl.

At potentials above the second oxidation observed in the CV of $\mathbf{20}^{4+}$ the most noticeable change was, again, a reduction in the intensity of the MLCT band, but on closer inspection the growth of a broad, lower intensity band at low energy was observed. Although the lower energy side of the band extends outside the range of the spectrometer, the band appeared to be Gaussian with a maximum ($\varepsilon \approx 3700$ dm^3 mol^{-1} cm^{-1}) centered at very low energy, *ca.* 2850 nm (~3500 cm^{-1}). The energy, intensity and form of this band are consistent with intervalence charge-transfer, IVCT. A comparison with the theoretical Hush model suggested that the complex is a Robin and Day Class II (valence trapped/electron hopping) system, perhaps verging on class II/III behaviour. Given that the previous studies demonstrated that $\mathbf{8}^{2+/3+}$ is a fully delocalized system, it is clear that substitution of the [RuCl([9]-ane-S_3] unit with [Ru([n]-ane-S_4] moieties results in a reduction in intermetallic coupling. The substitution of the π-donor chloride ligand with a π-accepting thiacrown-based sulfur ligand decreases the electron density on the metal center, thus stabilizing the Ru^{II} oxidation state. This results in the Ru^{II} metal centers accepting more electron density from the already electron deficient tetrazine ring of the bpta bridge, which destabilizes the oxidized form of the ligand with respect to the radical anion form. Increased back bonding also lowers electron density available for delocalization over the bridging ligand leading to a lowering of intermetallic electronic coupling. Surprisingly, no IVCT could be discerned when similar studies were carried out on **21**$^{4+}$, suggesting that the IVCT is still further shifted outside the window of the spectrometer used.

7. Dinuclear RuCl(n-S$_4$)-based complexes using bridging ligands with monodentate coordination sites.

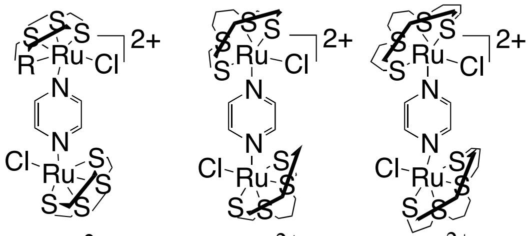

21^{2+} **22**$^{2+}$ **23**$^{2+}$

Figure 12 - Structures of dinuclear complexes, **22**$^{4+}$ - **24**$^{4+}$

With the aim of creating systems that were closer analogues of the original CT ion we synthesized complexes **22**$^{2+}$ - **24**$^{2+}$ in which RuCl(n-S$_4$) centers are bridged by pyrazine [44] – Figure 12. NMR data on all the three complexes and the crystal structures of **22**$^{2+}$ and **24**$^{2+}$ confirmed that these complexes take up a *cis*-geometry. Their oxidation was found to take place in two steps and again the dI$_1$/dE *vs*. E deconvolutions of the cv data facilitated an analysis of the data: as for complexes **17**$^{4+}$ - **19**$^{4+}$, the first Ru$^{III/II}$ couple for all the complexes displays good reversibility, while the second oxidation is not completely chemically reversible – Figure 13. Calculated K$_c$ values obtained from these data suggest that electrochemical coupling within **23**$^{3+}$ (K$_c$ = 75) is slightly higher than for **22**$^{3+}$ and **24**$^{3+}$ (K$_c$ = 35 for both), however - like the 9-S$_3$-based mixed donor set systems **6**$^{2+}$ - **8**$^{2+}$ - the apparent electrochemical interaction between the metal centers of the pyrazine bridged systems are considerably lower than those reported for N-donor systems such as the Creutz-Taube ion, where $K_c > 10^6$; but, again like **6**$^{3+}$ - **8**$^{3+}$, optical studies revealed contrasting results.

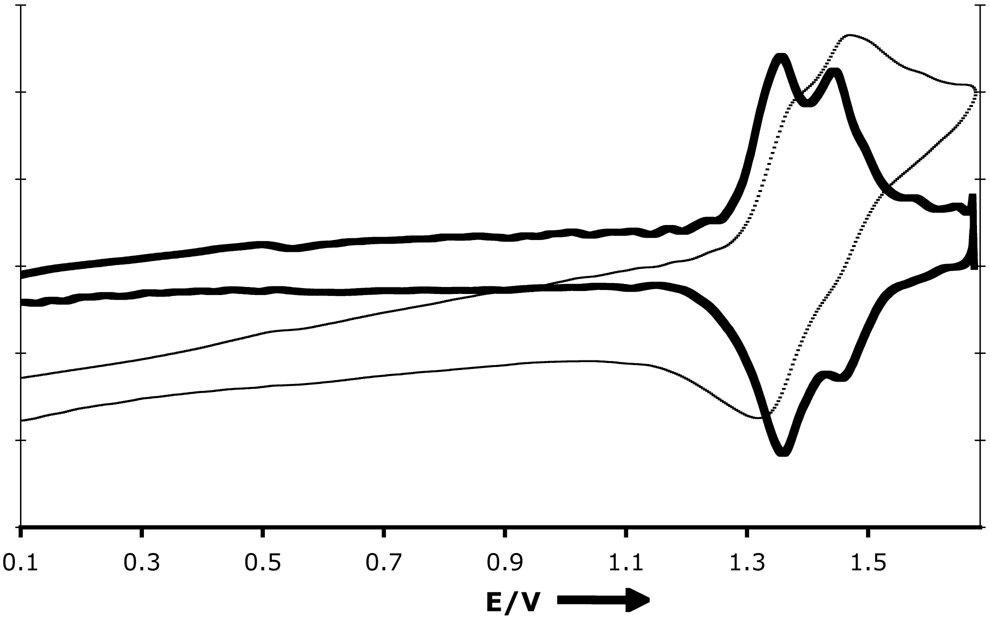

Figure 13 - Metal based oxidation couples for **21**$^{2+}$**.** Cyclic voltammogram (fine line) and dI1/dE vs. E deconvolutions (bold line).

The first one electron oxidation of all three complexes results in the growth of characteristic IVCT bands whose energy and shape are dependent on the identity of the coordinated thiacrown ligand. While the IVCT bands for **23**$^{3+}$ and **24**$^{3+}$ are symmetrical, the band for **22**$^{3+}$ is asymmetric with narrower half bandwidths on the high-energy side of the IVCT. Although IVCT band asymmetries are typical of the Class II/III interface where solvent interactions are averaged, these are observed at low energy [2]. Therefore it seems that - like the trinuclear systems discussed above - the asymmetry may arise from multiple IVCTs produced from Kramer doublets. A comparison of the IVCT data with the Hush model revealed disparities between experimental and calculated figures.

Complex **22**$^{3+}$ is the only one of the three systems with a $\Delta\nu_{1/2}$(calc) larger than the experimentally derived figure, indeed the value of $\Delta\nu_{1/2}$(expt) is probably slightly overestimated because – as outlined above - it is probably composed of several overlapping IVCTs. Contrastingly, for both **23**$^{3+}$ and **24**$^{3+}$ the experimentally observed

IVCT bands are appreciably wider than theoretical predictions, with this discrepancy being larger for **23**$^{3+}$ (~20%). This analysis suggests that although **22**$^{3+}$ is a Class III (valence delocalized), both **23**$^{3+}$ and **24**$^{3+}$ are valence localized Class II systems; it also indicates that – as in their RuCl(9-S$_3$) analogues – the low charge and combination of coordinated π-acceptor and π-donor ancillary ligands results in higher electronic coupling in the MV state than expected from the electrochemical data. Nevertheless, electronic coupling in these systems is still lower than that observed in the original CT-ion, which is a consequence of the π-accepting ability of the thiacrowns. Not only are the Ru^{II} oxidation couples for **22**$^{3+}$ - **24**$^{3+}$ anodically shifted compared to the CT ion, they are shifted compared to systems that incorporate typical π-accepting pyridyl-based ligands. Clearly, by accepting electron density from the metal centers, the coordinated thiacrown ligands lower delocalization across the bridging pyrazine; leading to an increased electron-transfer barrier and decreased electron transfer rate. To further investigate the experiment differences in electronic coupling between thiacrown-based systems computational studies on selected complexes were carried out

8. Computational studies

Using experimental X-ray data as a starting point, complexes **8**$^{2+}$, **17**$^{4+}$, **22**$^{2+}$, and **24**$^{2+}$ were fully optimized and compared at the DFT (B3LYP) level of theory [44]. As would be expected, for all the complexes, the HOMOs are out-of-phase metal centered orbitals and the LUMOs are π* orbitals localized on the bridging ligand – Figure 14. The most obvious difference between the systems occurs on replacing monodentate bridging ligands of **22**$^{2+}$ and **24**$^{2+}$ with the bidentate bridges of **8**$^{2+}$, **17**$^{4+}$ which leads to a > 20% increased participation of the metal ion the LUMO of the complex. A closer analysis also reveals differences in MO compositions due to the nature of the thiacrown.

A comparison of **22**$^{2+}$ with **24**$^{2+}$ shows that exchanging coordinated 12-S$_4$ with 16-S$_4$ causes a ~17% to ~13% *decrease* in the metal ion participation in the LUMO, furthermore the calculated ruthenium charges for **22**$^{2+}$ are -0.600 and -0.602, whilst for **24**$^{2+}$ the corresponding figures are -0.588 and -0.588; although these differences are small they suggest that the metal centers of **22**$^{2+}$ are slightly more electron rich than those of **3**$^{2+}$. DFT optimizations were also carried out on the **22**$^{2+}$ and **24**$^{2+}$ MV states, and the optical properties of the isovalent and MV systems were then investigated through TD-DFT.

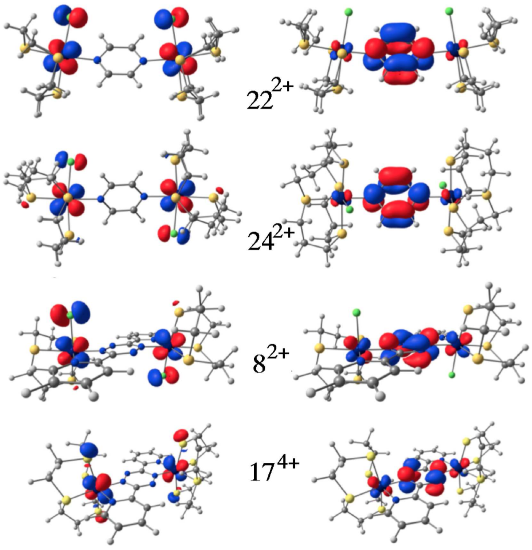

Figure 14 - HOMOs (left) and LUMOs (right) of complexes **22**$^{2+}$, **24**$^{2+}$, **8**$^{2+}$, and **17**$^{4+}$.

For both the isovalent states, the two strongest low-energy calculated transitions are Ru^{II}→pyrazine MLCT-based absorptions between 400 – 515 nm and, whilst the experimental data only displays a single absorption, it is consistent with an imposition of the calculated transitions. Strikingly, the calculated TD-DFT spectrum for the corresponding MV states leads to a different much lower energy excitation. As shown in Figure 15, this transition, which involves ruthenium-based orbitals on both metal centers, is clearly consistent with the postulated metal-to-metal charge-transfer. Further evidence of charge delocalization came from a Mulliken Population Analysis of spin densities: for both complexes the spin densities at *each* ruthenium center were equal. This latter analysis is slightly inconsistent with the experimental data indicating that only **21**$^{3+}$ is fully delocalized, however it is known that DFT overestimates delocalization of the unpaired electron due to self-repulsion effects [44].

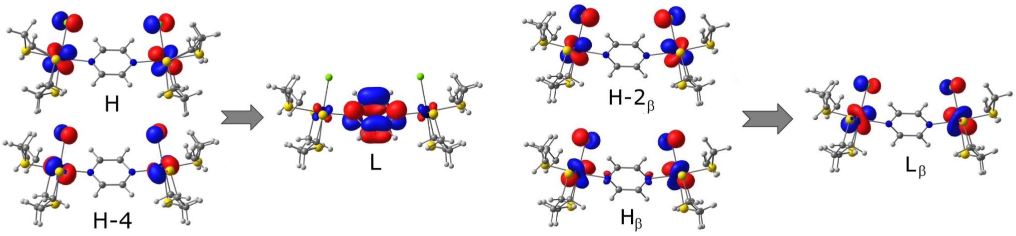

Figure 15. Kohn–Sham molecular orbitals involved in the electronic transitions of isovalent **21**$^{2+}$ (left) and its oxidized mixed valence analogue **21**$^{3+}$ (right).

9. Conclusions and future work

Due to their characteristic donor capabilities, thiacrown ligands produce distinctive effects on coordinated Ru^{II} centers, with both electronic and chemical properties being modulated relative to N-donor ligand sets. The electrochemical studies outlined in this review confirm that these macrocycles are strongly π-accepting. This can lead to dinuclear complexes in unusual redox states, as illustrated by the facile generation of the radical anion bridged **20**$^{3+}$ and **21**$^{3+}$ systems. The studies on the S_4 thiacrown-based MV complexes also illustrate how the nature of the coordinated ligand can subtly modulate the electrochemical *and* electronic properties of these systems. While the strong back bonding properties of the thiacrown ligands generally lower delocalization across the bridging ligand, perhaps the most interesting effects on electronic coupling arise in the lower charged complexes containing a mixture of thiacrown and π-donor ligands; for both S_3 and S_4 based complexes these conditions produce systems in which electrochemical data underestimates the true extent of electronic coupling. In future reports the effect of coordination to non-innocent redox active ligands in mono- and oligonuclear complexes involving relate thiacrown based centers will be explored.

Electronic effects involving coordinated 9-S3 also explain why ruthenium(II) centers coordinated to this ligands are anomalously labile for low-spin d^6-systems. This effect has been exploited to construct trinuclear supramolecular bowls possessing four accessible redox states. The distinctive connectivities in these bowls have resulted in MV states with unique electron-transfer properties. Studies on the host-guest properties of these systems will form the basis of forthcoming reports.

Acknowledgements. The quality of the work outlined in this review has been greatly enhanced through extremely fruitful collaborations with the groups of Prof. Mike D Ward here in Sheffield and Prof Vitor Felix at the Universidade de Aveiro, Portugal. I gratefully acknowledge financial support from The Royal Society and EPSRC.

References

[1] C. Creutz, H. Taube, H. J. Am. Chem. Soc. 91 (1969) 3988; C. Creutz, H. Taube, H. J. Am. Chem. Soc. 95 (1973) 1086.

[2] Selected reviews: C. Creutz, Prog. Inorg. Chem. 30 (1983) 1; R. J. Crutchley, Adv. Inorg. Chem. 41 (1994) 273; W. Kaim, A. Klein, M. Glöckle, Acc. Chem. Res. 33 (2000) 755; K. D. Demadis, C. M. Hartshorn, T. J. Meyer, Chem. Rev. 101 (2001) 2655; B. S. Brunschwig, C. Creutz, N.Sutin, Chem. Soc. Rev. 31 (2002) 168; J. T. Hupp, in:. T. J.Meyer, J. A. McCleverty (Eds.) Comprehensive Coordination Chemistry II, Elsevier, Oxford, 2004, vol. 2, p. 709; D. M. D'Alessandro, F. R. Keene, Chem. Soc. Rev. 35 (2006) 424; D. M. D'Alessandro, F. R. Keene, Chem. Rev. 106 (2006) 2270; W. Kaim, B. Sarkar, Coord. Chem. Rev. 251 (2007) 584; W. Kaim, G. K. Lahiri, Angew. Chem. Int. Ed. 46 (2007) 1778.

[3] M. D. Ward, Chem. Soc. Rev. 24 (1995) 121.

[4] K. Prassides (Ed.), Mixed Valency Systems—Applications in Chemistry, Physics and Biology, Kluwer Academic Publishers, Dordrecht, 1991.

[5] V. Balzani, A. Credi, M. Venturi, Molecular Devices and Machines: Concepts and Perspectives for the Nanoworld, Wiley-VCH, Weinheim, 2003.

[6] S. B. Braun-Sand, O. Wiest, J. Phys. Chem. B. 107 (2003) 9624; H. Tannai, K. Tsuge, Y. Sasaki Inorg. Chem. 44 (2005) 5206.

[7] J. Otsuki, T. Akasaka, K. Araki, Coord. Chem. Rev. 252 (2008) 32.

[8] J. R. Bolton, N. Mataga, G. McLendon (Eds.) Electron transfer in Inorganic, Organic, and Biological systems, Advances in Chemistry Series, 228, American Chemical Society, Washington, DC, 1991;

[9] J. P. Launay, Chem. Soc. Rev. 30 (2001) 386.

[10] See for example: A. J. Blake, G. Reid, M. Schröder, J. Chem. Soc. Dalton. Trans. (1989) 1675.

[11] C. Landgrafe and W. S. Sheldrick, J. Chem. Soc., Dalton Trans. (1994) 1885.

[12] S. Roche, H. Adams, S. E. Spey, J. A. Thomas, Inorg. Chem. 39 (2000) 2385.

[13] I. R. Young, L. A. Ochrymowycz, D. B. Rorabacher, Inorg. Chem. 25 (1986) 2576.

[14] K. Brandt, K.; W. S. Sheldrick, J. Chem. Soc., Dalton Trans. (1996) 1237.

[15] F. Laurent, E. Plantalech, B. Donnadieu, A. Jiménez, F. Hernández, M. Martínez-Ripoll, M. Biner, A. Llobet. Polyhedron 18 (1999) 3321; X. Sala, I. Romero, M. Rodríguez, and A. Llobet, Inorg. Chem. 43 (2004) 5403.

[16] G. E. D. Mullen, M. J. Went, S. Wocaldo, A. K. Powell, P. J. Blower, Angew. Chem., Int. Ed. Engl. 36 (1997) 1205; G. E. D. Mullen, T. F. Fassler, M. J. Went, K. Howland, B. Stein, P. J. Blower, J. Chem. Soc., Dalton Trans. (1999) 3759.

[17] S. Roche, L. J. Yellowlees, J. A. Thomas, Chem. Commun. (1998) 1429.

[18] C. S. Araújo, M. G. B. Drew, V. Félix, L. Jack, J. Madureira, M. Newell, S. Roche, T. M. Santos, J. A. Thomas, L. Yellowlees, Inorg. Chem. 41 (2002) 2250.

[19] C. H. Braunstein, A. D. Baker, T. C. Strekas, H. D. Gafney, Inorg. Chem. 23 (1984) 857; R. R. Ruminski, T. Cockroft, M. Shoup, Inorg. Chem. 27 (1988) 4026.

[20] D. P. Rillema, K. B. Mack, Inorg. Chem. 21 (1982) 3849; R. R. Ruminski, J. D. Peterson, Inorg. Chem. 21 (1982) 3706.

[21] J. E. B. Johnson, C. de Groff, R. R. Ruminski, Inorg. Chem. Acta 187 (1991) 73; J. Poppe, M. Moscherosch, W. Kaim, Inorg. Chem. 327 (1993) 2640.

[22] S. Ernst, V. Ksack, W. Kaim, Inorg. Chem. 27 (1988) 1146; W. Kaim, S. Ernst, V. Ksack, J. Am. Chem. Soc. 112 (1990) 173.

[23] B. D. Yeomans, D. G. Humphrey, G. A. Heath, Dalton Trans, (1997) 4153.

[24] F. Barriere, N. Camire, W. E. Geiger, U. T. Mueller-Westerhoff, R. Sanders, J. Am. Chem. Soc. 124 (2002) 7262.

[25] D. M. D'Alessandro, F. R. Keene, Dalton, Trans. (2004) 3950.

[26] N. S. Hush, Prog. Inorg. Chem. 8 (1967) 391.

[27] N. S. Hush, Electrochim. Acta 13 (1968) 1005.

[28] N. S. Hush, Coord. Chem. Rev. 64 (1985) 135.

[29] M. B. Robin, P. Day, Adv. Inorg. Chem. Radiochem. 10 (1967) 247.

[30] J. E. Sutton, H.Taube, Inorg. Chem. 20 (1981) 3125.

[31] S. Ferrere, C. M. Elliott, Inorg. Chem. 34 (1995) 5818.

[32] J. Thomas, Chem. Rev. 36 (2007) 856.

[33] S. Roche, C. Haslam, H. Adams, S. L. Heath, J. A. Thomas, Chem. Commun. (1998) 1429.

[34] See: R. H. Fish, Coord. Chem. Rev. 185–186 (1999) 569, and references therein.

[35] N. Shan, S. J. Vickers, H. Adams, M. D. Ward, J. A. Thomas, Angew. Chem. Int. Ed. 43 (2004) 3938.

[36] M. A. Bennett, L. Y. Goh and A. C. Willis, J. Chem. Soc., Chem. Commun. (1992) 1180; K. Brandt and W. S. Sheldrick, J. Chem. Soc., Dalton Trans. (1996) 1237.

[37] N. Shan, J. D. Ingram, T. L. Easun, S. J. Vickers, H. Adams, M. D. Ward, J. A. Thomas, Dalton Trans. (2006) 2900.

[38] J.-C. Imbeau and J.-M. Saveant, J. Electroanal. Chem. 44 (1973) 169; A. J. Bard, L.R. Faulkner, Electrochemical Methods. Fundamentals and Applications, Wiley, New York, USA, 2nd edn, 2001.

[39] S. Kar, T. A. Miller, S. Chakraborty, B. Sarkar, B. Pradhan, R. K. Sinha, T. Kundu, M. D. Ward, G. K. Lahiri, Dalton Trans. (2003) 2591; S. Patra, B. Sarkar, S. Ghumaan, J. Fiedler, W. Kaim, G. K. Lahiri, Dalton Trans. (2004) 754; D.M. D'Alessandro, M.S. Davies, F.R. Keene, Inorg. Chem. 45 (2006) 1656; C. S. Grange, A. J. H. M. Meijer, M. D. Ward, Dalton Trans. 39 (2010) 201.

[40] T. M. Santos, B. J. Goodfellow, J. Madureira, J. Pedrosa de Jesus, V. Felix, M. G. B. Drew, New J. Chem. 23 (1999) 1015.

[41] H. Adams, A. M. Amado, V. Félix, B. E. Mann, J. Antelo-Martinez, M. Newell, P. J. A. Ribeiro-Claro, S. E. Spey, J. A. Thomas, Chem. Eur. J. 11 (2005) 2031.

[42] M. Newell, J. A. Thomas, Dalton Trans (2006) 705.

[43] M. Newell, J. D. Ingram, T. L. Easun, S. Vickers, H. Adams, M. D. Ward, J. A. Thomas, Inorg. Chem. 45 (2006) 821.

[44] H. Adams, P. J. Costa, M. Newell, S. J. Vickers, M. D. Ward, V. Félix, J. A. Thomas, Inorg. Chem. 47 (2008) 11633.